SPECT/CT MIBG Imaging Is Crucial in the Follow-up of the Patients With High-Risk Neuroblastoma

Bin Liu, MD, PhD,† Sabah Servaes, MD,† and Hongming Zhuang, MD, PhD, FACNM†*

Background: Planar whole-body imaging with ^{123}I-radiolabeled metaiodobenzylguanidine (^{123}I-MIBG) is routinely used in the follow-up evaluation of neuroblastoma. In recent years, SPECT with integrated low-dose CT (SPECT/CT) has become more accessible. We investigated how much SPECT/CT can have additional diagnostic value over planar imaging in detection of residual and recurrent neuroblastoma.

Methods: A total of 170 planar ^{123}I-MIBG imaging scans with SPECT/CT follow-up scans performed in 147 patients with known high-risk neuroblastoma were retrospectively analyzed. Regions of increased ^{123}I-MIBG uptake on planar images and the findings on SPECT/CT were compared.

Results: In 61% of the studies, the whole-body planar images and SPECT/CT images yielded the same result. In 39% of the time, however, SPECT/CT images provided additional information.

Conclusions: In the follow-up of patients with high-risk neuroblastoma, SPECT/CT can significantly improve planar imaging interpretation and impact patient management.

Key Words: ^{123}I-MIBG, Neuroblastoma, SPECT/CT

(*Clin Nucl Med* 2018;43: 232–238)

Neuroblastoma is the most common extracranial solid tumor in childhood and accounts for approximately 15% of cancer deaths in children. It has been reported that tumor burden during and after multimodal treatment is strongly correlated with outcome in patients with neuroblastoma.[1–4] Therefore, accurate reevaluation of disease extent during and after treatment becomes crucial for the management of neuroblastoma because it may determine the prognosis for survival, the appropriate further treatment, and follow-up strategy.[5]

Metaiodobenzylguanidine (MIBG), a guanethidine analog, is essential in theranostics of neuroblastoma.[6–10] Metaiodobenzylguanidine radiolabeled with ^{123}I (^{123}I-MIBG) offers high-quality images and is widely used in the evaluation of patients with neuroblastoma.[11] Beyond usefulness in diagnosis and initial staging of neuroblastoma, ^{123}I-MIBG imaging is also helpful in gauging therapeutic decisions at points during treatment and monitoring patients who have completed treatment.[12] The lesions detected by MIBG scan at both diagnosis and postchemotherapy correlate with the prognosis.[1,2,13–15] Furthermore, ^{123}I-MIBG imaging is an essential tool in monitoring recurrent disease in patients who have achieved remission.

As the intrinsic nuclear scintigraphic characteristics, the assessment of conventional planar ^{123}I-MIBG images presents some difficulties. The limited resolution of planar images can induce false-negative results for small lesions,[16,17] whereas the presence of physiologic or nonneoplastic MIBG uptake is not always easily differentiable from pathologic uptake and can induce false-positive results. In addition, in planar images, lack of anatomic landmarks somewhat complicates interpretation of the images.[18]

SPECT/CT hybrid imaging technique, allowing the direct fusion of morphologic information and functional information, has been suggested to be more accurate.[19,20] However, SPECT/CT imaging renders slightly more radiation to patients from the CT portion of the study. In addition, the SPECT/CT imaging is time consuming, which not only significantly increases the workload of the technologists but also increases the necessity of sedating patients, especially toddlers. For these reasons, it remains not universally agreed whether SPECT/CT images should be acquired in the evaluation of possible recurrent neuroblastomas.

In the present study, we attempted to investigate how much additional value SPECT/CT may have over conventional planar ^{123}I-MIBG whole-body imaging in detecting and characterizing residual and recurrent neuroblastomas.

MATERIALS AND METHODS

Patients

In our study, we retrospectively investigated a total of 147 consecutive patients (69 boys, 78 girls; mean age, 4.3 ± 3.9 years) with histologically proven neuroblastoma who had both ^{123}I-MIBG static imaging and SPECT/CT imaging. These patients were referred either for the response evaluation routinely performed at points during treatment or for the surveillance of local recurrence or distant metastases during long-term follow-up. Patients with non–MIBG-avid tumors were excluded from the analysis.

Overall, a total of 170 paired scans (13 patients had undergone scans twice, and 5 patients had 3 repeat scans over the course of their diseases) were analyzed. The investigation was approved by the institutional review board, and the requirement of written informed consent was waived.

Imaging Protocol

All patients underwent the routine ^{123}I-MIBG imaging, including thyroid blockage with potassium iodide before and for 2 days after ^{123}I-MIBG administration. Approximately 24 hours after intravenous administration of ^{123}I-MIBG (5.2 MBq/kg) with a maximum of 370 MBq and a minimum of 37 MBq,[21] planar whole-body imaging was performed in both anterior and posterior projections using the gamma camera component of the hybrid cameras (Symbia T2; Siemens Healthcare, Malvern, PA) equipped with low-energy general-purpose collimators. Immediately after planar imaging, a SPECT/CT imaging was acquired. SPECT/CT view was focused

Received for publication December 26, 2017; revision accepted December 29, 2017.
From the *Department of Nuclear Medicine, West China Hospital, Sichuan University, Chengdu, Sichuan, China; and †Department of Radiology, Children's Hospital of Philadelphia, University of Pennsylvania School of Medicine, Philadelphia, PA.
Conflicts of interest and sources of funding: This work was in part supported by the grant from China Scholarship Council (no. 2011624088) and national fund of nature and science (no. 81401445) to B.L. None declared to all other authors.
Correspondence to: Hongming Zhuang, MD, PhD, FACNM, Department of Radiology, Children's Hospital of Philadelphia, University of Pennsylvania School of Medicine, 34th & Civic Ctr Blvd, Philadelphia, PA 19104. E-mail: zhuang@email.chop.edu.

ISSN: 0363-9762/18/4304–0232
DOI: 10.1097/RLU.0000000000001984

on suspected areas of increased uptake as seen on planar images. For cases with negative findings on planar imaging, SPECT/CT was focused on the previously abnormal MIBG uptake areas on prior pretherapy studies or medical record. The SPECT imaging was followed by a low-dose CT, which was acquired for attenuation correction and localization purpose. SPECT images were reconstructed with the iterative method and fused with CT images using the Syngo MI Applications software (Siemens Medical Solutions, Malvern, PA).

Data Analysis

All images were individually viewed by 2 nuclear medicine physicians. Consensus interpretation was obtained by both readers if there was any initial different interpretation. Planar images were assessed first. Any uptake with its intensity greater than background activity and incompatible with normal distribution was considered to be abnormal. Planar images were considered equivocal when it was not easy to ascertain the anatomic site or to characterize the foci of MIBG uptake. The SPECT/CT fusion images were considered contributory if they gave better identification and interpretation of the hot spots, more accurate anatomic localization and characterization, precise discrimination between tumor lesions and physiologic distributions, and detection of a greater number of tumor deposits when not obtained from the planar images.

Standard of Truth

The presence or absence of tumor was established in at least one of the following methods: (*a*) histopathologic diagnosis; (*b*) other diagnostic imaging less than 14 days with ^{123}I-MIBG imaging, including contrast-enhanced CT, MRI, ^{18}F-FDG PET/CT, and posttherapy therapeutic ^{131}I-MIBG imaging; (*c*) clinical follow-up from 1 to 23 months.

RESULTS

From the total 170 paired comparison between the whole-body static images and SPECT/CT images, 61% (104 of 170) of the studies were consistent, and SPECT/CT images simply confirmed the findings revealed on static images. However, in the remaining 39% (66 of 170) of the studies, SPECT/CT provided additional information that enabled more accurate diagnosis than that from static images.

SPECT/CT Images Increased the Sensitivity of the Study

Among these 66 studies, SPECT/CT images detect lesions unrecognizable on static images in 33 of them. These are especially true when the lesions are at locations with overlapping organs, which can have relatively high physiological MIBG activity, including kidney (Fig. 1), urinary bladder (Fig. 2), or the heart (Fig. 3).

SPECT/CT Increased the Confidence of the Image Interpretation

In addition, SPECT/CT images gave a definite diagnosis in 23 studies where the interpretation of static images was either inconclusive (Fig. 4) or unconvincing to referring physicians (Fig. 5).

SPECT/CT Increased Specificity of the Study

Furthermore, the SPECT/CT correctly identified 7 cases of increased uptake caused by nonmalignant etiologies, which was thought to be recurrent disease based on planar images (Figs. 6 and 7).

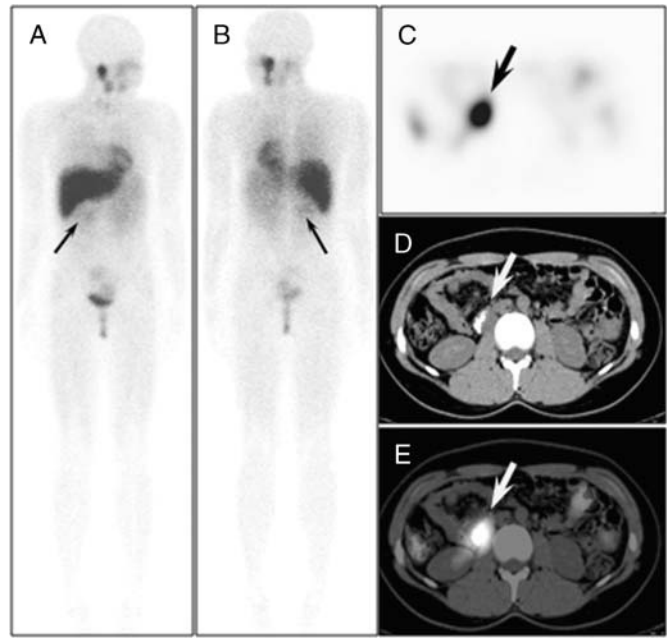

FIGURE 1. A ^{123}I-MIBG scan was performed in a 12-year-old girl with a treated high-risk neuroblastoma to determine whether there was any MIBG-avid recurrent disease. Both anterior (**A**) and posterior (**B**) whole-body images showed relatively normal tracer distribution. Mild activity (arrows) overlapping the renal fossa was thought to represent radioactive urine in the kidney. However, on the axial SPECT (**C**), CT (**D**), and fusion (**E**) images, there was an intense activity (arrow) in a partially calcified right retroperitoneal soft tissue mass, which was subsequently proven to be neuroblastoma by histopathologic examination.

In 3 cases, the SPECT/CT more accurately localized lesions than the planar images (Figs. 8 and 9).

DISCUSSION

As a useful diagnostic noninvasive imaging procedure, SPECT/CT provides excellent images, the use of which can guide management in patients with both oncological and nononcological conditions.[19,20] Further, there is emerging literature that demonstrates that MIBG SPECT/CT may improve localization and characterization of neuroblastoma. Fukuoka et al[18] compared the diagnostic value of SPECT/CT and planar imaging in 8 patients with pheochromocytomas and 8 patients with neuroblastomas using ^{123}I-MIBG and posttherapy therapeutic ^{131}I-MIBG. It was shown that ^{123}I-MIBG SPECT/CT offered additional information to planar imaging in 81% of the studies and for 75% of the patients. In a retrospective study by Rozovsky et al,[23] analyzing the impact of SPECT/CT on correlation of ^{131}I-MIBG imaging and diagnostic CT in 8 patients with neuroblastoma and 3 patients with pheochromocytoma, SPECT/CT was suggested to bridge the gap between the 2 imaging techniques by increasing the diagnostic certainty in 89% of discordant studies. Pfannenberg et al.[24] reported that SPECT/CT fused images changed therapy plans in 14 (28%) of the 50 patients with various neuroendocrine tumors using ^{111}In-octreotide and ^{123}I-MIBG. However, these studies were often limited by heterogeneous study populations with limited number of patients with neuroblastoma recruited. The results of our study exploring the value of ^{123}I-MIBG SPECT/CT in a larger cohort of 170 paired scans from 147 patients with neuroblastoma

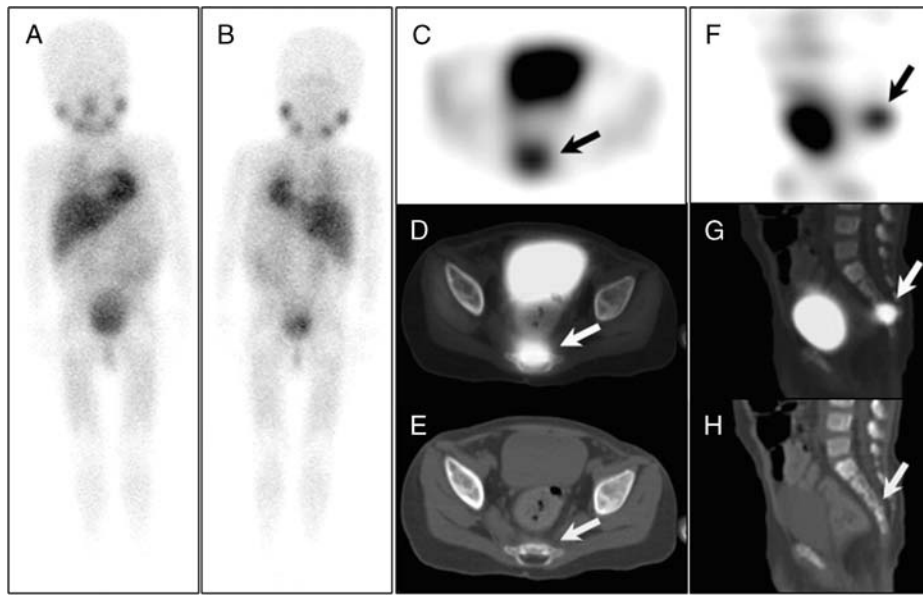

FIGURE 2. A 3-year-old boy was found to have a left adrenal mass, which was resected and confirmed as high-risk neuroblastoma pathologically. Eight months after surgery and 1 month after the completion of chemotherapy, he was transferred to our hospital for further evaluation. A ^{123}I-MIBG scan with SPECT/CT images of the abdomen and pelvic was ordered by referring physician for restaging. The tracer distribution in the whole-body planar image (**A**, anterior; **B**, posterior) was unremarkable. However, on both axial (**C**, SPECT; **D**, fusion; **E**, CT) and sagittal (**F**, SPECT; **G**, fusion; **H**, CT) SPECT/CT images, an intense activity was noted in S3–4 vertebrae with sclerotic changes on CT images, consistent with osseous metastasis. The false-negative interpretation of the whole-body images was due to overlapping radioactive urine in the bladder, which prevented the sacral lesion from being visualized on whole-body images.

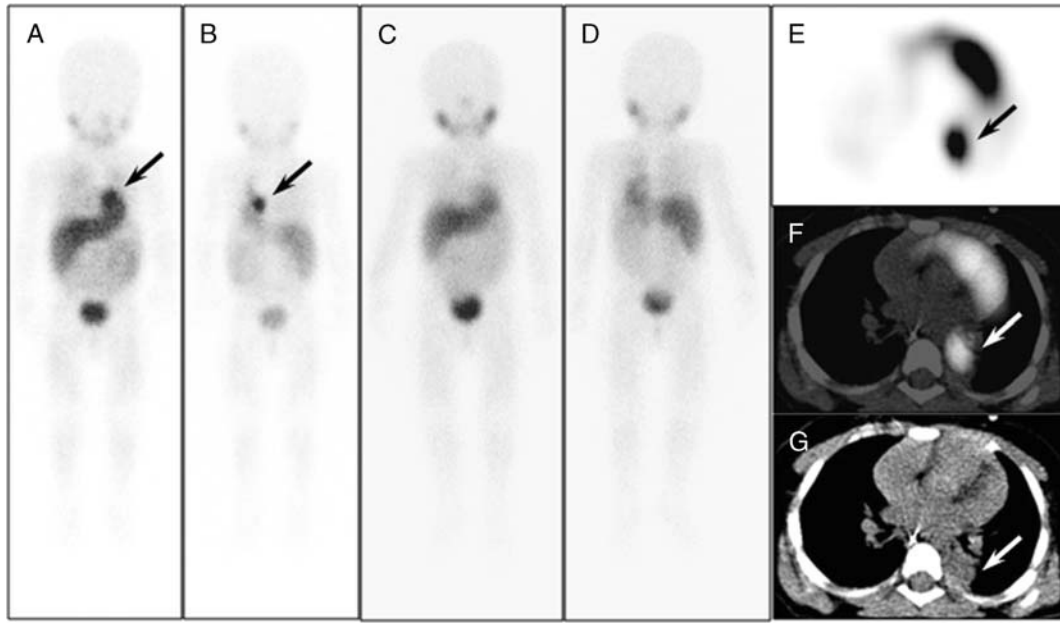

FIGURE 3. A 15-month-old girl was diagnosed as having left-chest paraspinal neuroblastoma, which showed intense activity on the initial staging ^{123}I-MIBG whole-body images (arrows, **A**, anterior; **B**, posterior view). Following therapy, a restaging whole-body ^{123}I-MIBG scan (**C**, anterior; **D**, posterior) performed 6 months after initial MIBG study revealed no definite evidence of abnormal MIBG activity. However, on axial SPECT (**E**) and fusion (**F**) images, the abnormal activity (arrows) in the posterior left chest was clearly visualized, which corresponded to left paraspinal soft tissue mass (arrow) on the low-dose CT image (**G**). The cause of the false-negative reading on whole-body images was due to the relatively reduced activity of the lesion after therapy, which overlapped the normal cardiac MIBG activity.[22]

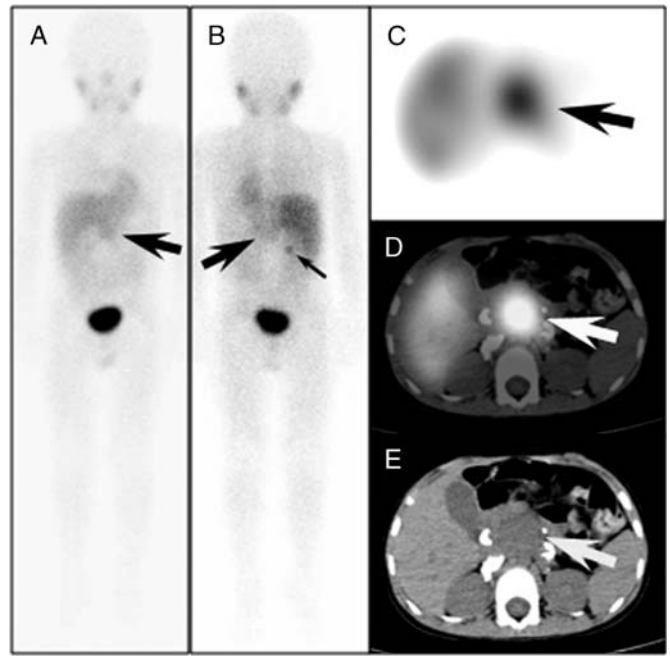

FIGURE 4. A 4-year-old boy was transferred to our hospital from an outside institution. He suffered abdominal neuroblastoma with osseous metastasis 10 months prior and had received therapy. An MIBG scan was ordered for staging. The whole-body images (**A**, anterior; **B**, posterior) showed no abnormal activity in the bones. There was a small focal activity in the right renal fossa (small arrow), which was regarded as urine activity in the right renal pelvis. In addition, there was a large region of mildly increased activity (large arrows) in the midline upper abdomen with its intensity not higher than the level of the liver. Because soft tissue lesions from neuroblastoma commonly have higher MIBG activity than physiological liver uptake, the findings from the whole-body images were uncertain. However, on SPECT/CT images (**C**, SPECT; **D**, fusion; **E**, CT), the activity (arrows) was clearly more intense than the liver activity and corresponded to a soft tissue mass that measured approximately $4 \times 4 \times 5$ cm. The SPECT/CT images were consistent with MIBG-avid malignancy.

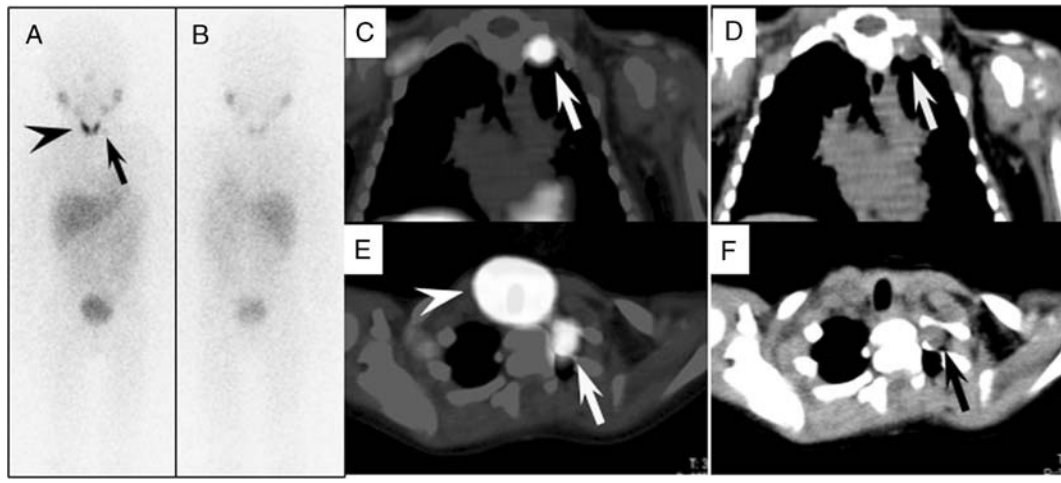

FIGURE 5. A 6-month-old girl showed irritability for 3 weeks. Physiological examination revealed lower-extremity neurological compromise, which prompted MRI examination and eventually led to diagnosis of T-spine neuroblastoma. Her primary tumor was resected. She also received chemotherapy, and a remission was achieved. At the age of 3 years, she underwent a routine surveillance ^{123}I-MIBG study. The whole-body images (**A**, anterior; **B**, posterior) did not reveal any obvious abnormal activity. Intense activity was noted in the region of the thyroid (arrowhead), which was attributed to the free-iodine activity. In addition, very subtle activity (arrow) was noted in the region lateral to the lower pole of the left lobe of the thyroid, which could be easily missed by inexperienced readers. However, on both coronal (**C**, fusion; **D**, CT) and axial (**E**, fusion; **F**, CT) images, this activity (arrows) corresponded to a partially calcified soft tissue mass in the left apex of the lung, which has intensity only slightly less than the thyroid activity (arrowhead, **E**). The findings were consistent with recurrent malignancy, which was confirmed by subsequent pathological examination.

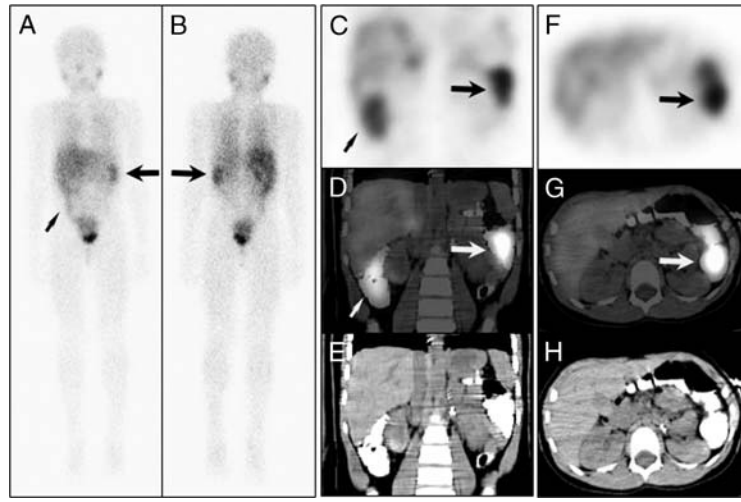

FIGURE 6. A 2-year-old boy had high-risk stage IV neuroblastoma diagnosed from an outside institution. His primary left adrenal tumor was resected. After completion of chemotherapy for his diffuse bone metastases, he was transferred to our hospital. The whole-body images (**A**, anterior; **B**, posterior) showed no abnormal activity at the site of the left adrenal or any bones. Linear activity with its intensity less than the liver was noted in the right lower abdomen (thin arrow), which was commonly seen as intestinal activity. However, there was a focal activity (thick arrow) with its intensity higher than the liver in the left upper abdomen on both anterior and posterior views, which raised possibility of MIBG-avid soft tissue mass. However, on the coronal (**C**, SPECT; **D**, fusion; **E**, CT) and axial (**F**, SPECT; **G**, fusion; **H**, CT) images, both the right lower abdominal linear activity (thin arrows) and the left upper quadrant activity (thick arrows) corresponded to high-density oral CT contrast inside the colon. The findings excluded recurrent disease. The subsequent follow-up showed no evidence of residual or recurrent disease.

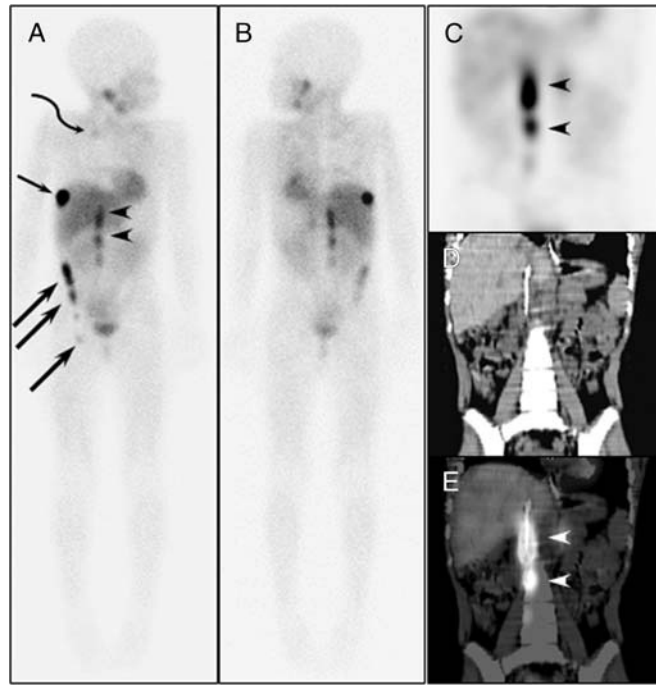

FIGURE 7. A ^{123}I-MIBG scan was performed to monitor high-risk neuroblastoma in a 7-year-old girl who had her primary tumor resected from the right upper chest 1 year prior. The whole-body image (**A**, anterior; **B**, posterior) revealed multiple foci of intense activity in the right side of her body, corresponding to the known Port-A-Cath (small arrow) and related intravenous line outside the body (large arrows), as a result of poor tracer injection. The subtly increased activity in the right apex of the lung (curved arrow) was consistent with residual/recurrent tumor. However, there were also several foci of intense activity in the midline lower thorax and upper abdomen in a vertically linear pattern (arrowheads), which were new and of unknown etiology based on whole-body images. The coronal SPECT/CT images (**C**, SPECT; **D**, CT; **E**, fusion) clearly showed that the activity was in the central line (arrowheads) in the inferior vena cava and not soft tissue lesion.

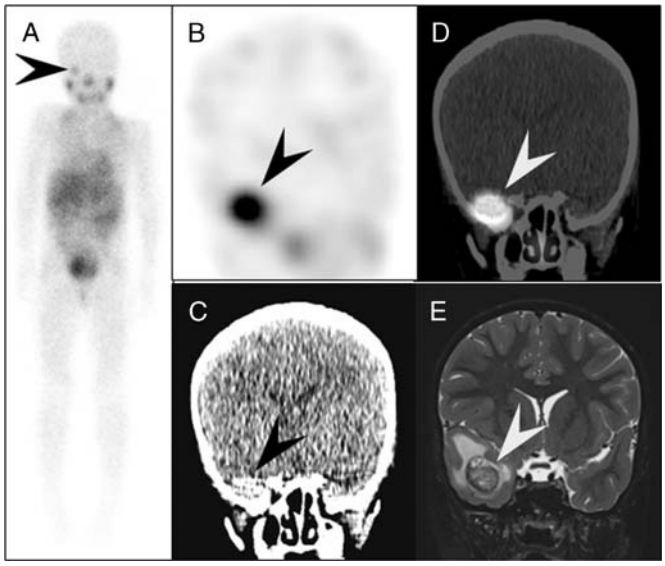

FIGURE 8. A 6-year-old asymptomatic girl in presumed remission underwent a surveillance ^{123}I-MIBG scan for high-risk neuroblastoma she had 2 years prior. Her primary right adrenal tumor had been resected. She also underwent chemotherapy, immunotherapy, and autologous stem cell transplantation. The MIBG scan at the completion of the therapy showed no evidence of MIBG-avid disease. The current whole-body image (**A**, anterior view) showed largely normal tracer distribution except for 1 focus of increased activity in the right orbital region (arrowhead), which is a common site of bone metastasis from neuroblastoma. On coronal SPECT/CT images (**B**, SPECT; **C**, CT brain window; **D**, fusion), however, this activity (arrowheads) not only was located in the right sphenoid bone but also invaded adjacent brain cortex, which was partially calcified (**C**, arrowhead). The brain involvement was subsequently confirmed by a brain MRI study (**E**, coronal T2 weighted, arrowhead). The patient received proton therapy to the right sphenoid/temporal brain lesion and responded well. Three separate follow-up MIBG studies were all negative.

confirm that the diagnostic performance of ^{123}I-MIBG planar imaging is improved by SPECT/CT in detection of recurrent and metastatic neuroblastoma.

In our study, the diagnosis reached by planar imaging was revised or specified by SPECT/CT in 66 (39%) of the 170 studies. SPECT/CT studies can confidently detect abnormal lesions that were missed on planar images because of either the small size or overlapping physiological activity. Another major advantage of SPECT/CT was noted for exclusion of suspicion of disease suggested by planar MIBG imaging, thus improving the specificity of planar MIBG imaging. MIBG imaging has high specificity for neuroblastoma, yet false-positive results can still be seen,[25–37] especially on planar images. As a consequence of better lesion detectability offered by SPECT/CT, the disease could be reclassified; the more appropriate therapeutic protocol selected, the more proper prognosis determined. This was particularly relevant in those cases in whom the occult MIBG-avid lesions were the only ones detected (Figs. 1, 2, and 8).

In summary, SPECT/CT led to more accurate assessment of response, better planning of treatment strategies, earlier detection of recurrence disease, and the avoidance of unnecessary treatment. The capability of SPECT/CT to more accurately define the abnormal activity justifies the additional use of low-dose CT. The hypothetical risk attributable to additional radiation is very small compared with the obvious benefits brought by SEPCT/CT, especially in patients with high-risk neuroblastoma in whom precise delineation of disease extent is extremely important.

CONCLUSIONS

The information from ^{123}I-MIBG SPECT/CT imaging led to more accurate assessment of residual or recurrent high-risk neuroblastoma in approximately 2 of 5 patients in our investigation and could significantly impact the patients' management. The potential benefit-risk ratio from performing SPECT/CT is high in monitoring patients with treated high-risk neuroblastomas.

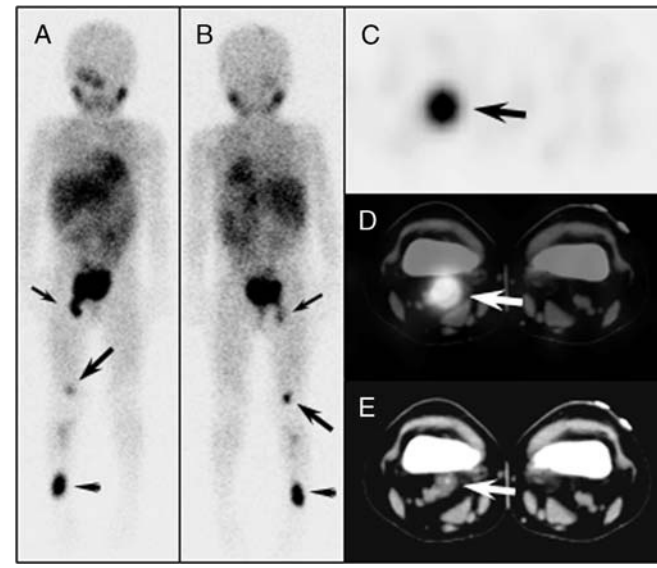

FIGURE 9. A 2-year-old girl underwent an MRI of the distal lower extremity to evaluate possible osteomyelitis due to lower leg pain. The images (not shown) showed diffuse bone marrow signal abnormality in bilateral distal femora, tibias, and fibulas without any lymph node abnormality. The diffuse bone marrow abnormality did not support osteomyelitis but suggested a bone metastatic disease. A right adrenal primary neuroblastoma with diffuse bone metastases was subsequently diagnosed. Primary tumor was surgically resected, and chemotherapy was initiated. A posttherapy restaging ^{123}I-MIBG scan (**A**, anterior view; **B**, posterior view) showed cluster of abnormal activity in the right inguinal region (thin arrows), consistent with lymph node involvement, which was known prior to the scan. In addition, there was also abnormal activity in the right orbital region, in the region of right distal femur (thick arrows), and in the right tibia, more intense in the distal right tibia (arrowheads). However, the activity in the region of the distal right femur appeared much less prominent on the anterior view (**A**) than on the posterior view (**B**), which was uncommon for a femoral lesion. SPECT/CT images of the femurs were subsequently acquired. On axial images (**C**, SPECT; **D**, CT; **E**, fusion), the activity (arrows) corresponded to a partially calcified enlarged popliteal lymph node, not the right femur. The planned external radiation regimen was consequently revised.

REFERENCES

1. Yanik GA, Parisi MT, Shulkin BL, et al. Semiquantitative mIBG scoring as a prognostic indicator in patients with stage 4 neuroblastoma: a report from the Children's oncology group. *J Nucl Med*. 2013;54:541–548.
2. Katzenstein HM, Cohn SL, Shore RM, et al. Scintigraphic response by ^{123}I-metaiodobenzylguanidine scan correlates with event-free survival in high-risk neuroblastoma. *J Clin Oncol*. 2004;22:3909–3915.
3. Maris JM. Recent advances in neuroblastoma. *N Engl J Med*. 2010;362: 2202–2211.
4. Maris JM, Hogarty MD, Bagatell R, et al. Neuroblastoma. *Lancet*. 2007;369: 2106–2120.
5. Park JR, Bagatell R, London WB, et al. Children's Oncology Group's 2013 blueprint for research: neuroblastoma. *Pediatr Blood Cancer*. 2013;60: 985–993.
6. Parisi MT, Eslamy H, Park JR, et al. ^{131}I-metaiodobenzylguanidine theranostics in neuroblastoma: historical perspectives; practical applications. *Semin Nucl Med*. 2016;46:184–202.
7. Kushner BH, Kramer K, Modak S, et al. Sensitivity of surveillance studies for detecting asymptomatic and unsuspected relapse of high-risk neuroblastoma. *J Clin Oncol*. 2009;27:1041–1046.
8. Johnson K, McGlynn B, Saggio J, et al. Safety and efficacy of tandem ^{131}I-metaiodobenzylguanidine infusions in relapsed/refractory neuroblastoma. *Pediatr Blood Cancer*. 2011;57:1124–1129.
9. Hickeson MP, Charron M, Maris JM, et al. Biodistribution of post-therapeutic versus diagnostic (131)I-MIBG scans in children with neuroblastoma. *Pediatr Blood Cancer*. 2004;42:268–274.
10. Yang J, Codreanu I, Servaes S, et al. I-131 MIBG post-therapy scan is more sensitive than I-123 MIBG pretherapy scan in the evaluation of metastatic neuroblastoma. *Nucl Med Commun*. 2012;33:1134–1137.
11. Liu B, Zhuang H, Servaes S. Comparison of [^{123}I]MIBG and [^{131}I]MIBG for imaging of neuroblastoma and other neural crest tumors. *Q J Nucl Med Mol Imaging*. 2013;57:21–28.
12. Boubaker A, Bischof Delaloye A. MIBG scintigraphy for the diagnosis and follow-up of children with neuroblastoma. *Q J Nucl Med Mol Imaging*. 2008;52:388–402.
13. Lewington V, Lambert B, Poetschger U, et al. ^{123}I-mIBG scintigraphy in neuroblastoma: development of a SIOPEN semi-quantitative reporting method by an international panel. *Eur J Nucl Med Mol Imaging*. 2017;44:234–241.
14. Decarolis B, Schneider C, Hero B, et al. Iodine-123 metaiodobenzylguanidine scintigraphy scoring allows prediction of outcome in patients with stage 4 neuroblastoma: results of the Cologne Interscore Comparison Study. *J Clin Oncol*. 2013;31:944–951.
15. DuBois SG, Mody R, Naranjo A, et al. MIBG avidity correlates with clinical features, tumor biology, and outcomes in neuroblastoma: a report from the Children's Oncology Group. *Pediatr Blood Cancer*. 2017.
16. Pirson AS, Krug B, Tuerlinckx D, et al. Additional value of I-123 MIBG SPECT in neuroblastoma. *Clin Nucl Med*. 2005;30:100–101.
17. Udall D, Cho SY. Congenital agenesis of right parotid gland confounds MIBG scan interpretation in craniocervical neuroblastoma. *Clin Nucl Med*. 2011; 36:e162–e164.
18. Fukuoka M, Taki J, Mochizuki T, et al. Comparison of diagnostic value of I-123 MIBG and high-dose I-131 MIBG scintigraphy including incremental value of SPECT/CT over planar image in patients with malignant pheochromocytoma/paraganglioma and neuroblastoma. *Clin Nucl Med*. 2011;36:1–7.
19. Buck AK, Nekolla S, Ziegler S, et al. SPECT/CT. *J Nucl Med*. 2008;49: 1305–1319.
20. Mariani G, Bruselli L, Kuwert T, et al. A review on the clinical uses of SPECT/CT. *Eur J Nucl Med Mol Imaging*. 2010;37:1959–1985.
21. Gelfand MJ, Parisi MT, Treves ST, et al. Pediatric radiopharmaceutical administered doses: 2010 North American consensus guidelines. *J Nucl Med*. 2011;52:318–322.
22. Chen W, Botvinick EH, Alavi A, et al. Age-related decrease in cardiopulmonary adrenergic neuronal function in children as assessed by I-123 metaiodobenzylguanidine imaging. *J Nucl Cardiol*. 2008;15:73–79.
23. Rozovsky K, Koplewitz BZ, Krausz Y, et al. Added value of SPECT/CT for correlation of MIBG scintigraphy and diagnostic CT in neuroblastoma and pheochromocytoma. *AJR Am J Roentgenol*. 2008;190:1085–1090.
24. Pfannenberg AC, Eschmann SM, Horger M, et al. Benefit of anatomical-functional image fusion in the diagnostic work-up of neuroendocrine neoplasms. *Eur J Nucl Med Mol Imaging*. 2003;30:835–843.
25. Schindler T, Yu C, Rossleigh M, et al. False-positive MIBG uptake in pneumonia in a patient with stage IV neuroblastoma. *Clin Nucl Med*. 2010;35: 743–745.
26. Pfluger T, Schmied C, Porn U, et al. Integrated imaging using MRI and ^{123}I metaiodobenzylguanidine scintigraphy to improve sensitivity and specificity in the diagnosis of pediatric neuroblastoma. *AJR Am J Roentgenol*. 2003; 181:1115–1124.
27. Acharya J, Chang PT, Gerard P. Abnormal MIBG uptake in a neuroblastoma patient with right upper lobe atelectasis. *Pediatr Radiol*. 2012;42:1259–1262.
28. Liu B, Yang H, Codreanu I, et al. Increased MIBG activity in the uterine cervix due to menstruation. *Clin Nucl Med*. 2015;40:179–181.
29. Bai X, Zhuang H. MIBG Activity in the Gallbladder. *Clin Nucl Med*. 2016; 41:576–577.
30. Bai X, Zhuang H. Focally increased MIBG activity in the muscle: real lesion or LOVENOX injection artifact? *Clin Nucl Med*. 2016;41:167–168.
31. Zhao X, Zhuang H. Variable MIBG activity in the same renal cyst. *Clin Nucl Med*. 2017;42:887–889.
32. Liu B, Codreanu I, Yang J, et al. Diffuse elevated MIBG activity in the renal parenchyma caused by compromised renal blood flow. *Clin Nucl Med*. 2014; 39:1005–1008.
33. Bai X, Zhuang H. Persistent asymmetric brain MIBG activity related to a cerebrovascular infarct. *Clin Nucl Med*. 2016;41:344–345.
34. Xie P, Monaghan R, Edwards K, et al. Elevated MIBG activity at the site of erythema of unknown etiology. *Clin Nucl Med*. 2017;42:227–230.
35. Granata C, Carlini C, Conte M, et al. False positive MIBG scan due to accessory spleen. *Med Pediatr Oncol*. 2001;37:138–139.
36. Moralidis E, Arsos G, Papakonstantinou E, et al. ^{123}I-metaiodobenzylguanidine accumulation in a urinoma and cortex of an obstructed kidney after surgical resection of an abdominal neuroblastoma. *Pediatr Radiol*. 2008;38:118–121.
37. Rottenburger C, Juettner E, Harttrampf AC, et al. False-positive radio-iodinated metaiodobenzylguanidine (^{123}I-MIBG) accumulation in a mast cell–infiltrated infantile haemangioma. *Br J Radiol*. 2010;83:e168–e171.